EMITTANCE PRESERVATION FOR THE ILC MAIN LINAC*

Kirti Ranjan#. Department of Physics & Astrophysics, University of Delhi, Delhi, India

Abstract

The luminosity performance of the proposed International Linear Collider (ILC) will be affected by many issues. This paper addresses issues associated with the emittance preservation in the main Linac, including static and dynamic imperfections, of the ILC machine. Preserving the ultra-small emittances requires component alignment tolerances far beyond that which can be achieved by traditional mechanical and optical alignment techniques, hence the use of beam-based alignment and tuning techniques are essential in obtaining the design luminosity. The performance of the ILC main linac has been simulated for a variety of errors (both static and dynamic) and beneficial effects of the beam based alignment techniques are discussed.

INTRODUCTION

One of the crucial accelerator design and operation issues for the proposed ILC machine would be the preservation of small transverse beam emittances in beam propagation through main linac. Because of the large aspect ratio in both spot size and emittance, challenges in the vertical plane would be at least an order of magnitude more difficult than in the horizontal plane. Various sources of emittance dilution in the main linac include dispersion originating from misaligned quadrupoles and BPMs, pitched cavities and cryomodules, wakefields generated from cavity offsets, and coupling between the transverse planes coming from rotated (or skew) quads. It is well established now that beam-based alignment (BBA) techniques in the main linac will be indispensable to limit the emittance growth to the desired small values. To this end, various static tuning algorithms were proposed, investigated, and developed over the last 15 years [1]. Dispersion Free Steering (DFS) was demonstrated to be one of the effective techniques in earlier NLC and TESLA studies and is also considered to be an attractive approach for the ILC main linac. It is thus important to analyze the performance of DFS in the main linac. In order to understand the stringency of the tolerance of a given beamline element it is crucial to study the sensitivity of the DFS algorithm to various misalignments and incoming beam and quad vibration jitter. The robustness of the DFS algorithm to a failure of a BPM or corrector is also considered. To increase robustness in the tuning options, emittance bumps are suggested as an effective means for emittance preservation. Simulation results on the effectiveness of these bumps are also presented.

However, it is also crucial that the achieved emittance budget should remain stable in the presence of ground motion and elements vibrations/jitter. It is certain that ground motion can severely affect the luminosity performance of the machine, and hence the machine should be dynamically aligned continuously in order to correct it. Adaptive alignment (AA) technique is one of the attractive tuning options as it relies only on the BPM readings. The algorithm was first proposed for the VLEPP project [2]. AA is a local method in which the BPM readings of the neighbouring quads are used to determine the necessary shifting of a central quad. The procedure is iteratively repeated to get the final solution.

In the main linac of the proposed ILC accelerator, which is filled with TESLA-type superconducting cavities, fundamental (Input) coupler & higher order mode (HOM) coupler cause asymmetric fields, which can adversely affect the luminosity at the interaction point (IP). Transverse kicks are of two types: Coupler RF kick which is due to asymmetry in fundamental RF fields & coupler transverse short-range wake fields which are generated by the beam even if the beam is on-axis. We calculate the emittance dilution in the main linac due to coupler RF kick and coupler wake kick.

ILC MAIN LINAC

The ILC main linac considered in this study is an adaptation from the design envisaged in the ILC BCD [3]. A fully loaded gradient of 31.5MeV/m is considered for the 9-cell 1.3 GHz accelerating cavities. The main linac cryogenic system is divided into cryomodules (CM), with 8 cavities per CM. A quad package consisting of a quadrupole magnet, a cavity-style BPM, and horizontal and vertical corrector magnets is installed in every fourth CM. The magnet optics is a FODO lattice with a phase advance per cell of 75^0 (60^0) in the horizontal (vertical) plane. The beam injection energy is 15 GeV, the extraction energy is 250 GeV, and the single bunch charge is 2×10^{10}. The nominal installation precision for various beamline elements are given in Table 1.

Table 1: RMS alignment tolerances for a curved ILC main linac in the vertical plane.

Misalignment	With respect to	Tolerance (μm)
Quad offset	CM	300
Quad rotation	CM	300
BPM resolution	-	1
BPM offset	CM	300
Cavity offset	CM	300
Cavity pitch	CM	300
CM offset	Survey Line	200
CM pitch	Survey Line	20

Simulations are performed using MatLIAR [4] and Lucretia [5]. In order to simulate the effect of the earth's

*Work supported by IUSSTF
#kranjan@physics.du.ac.in

curvature in MatLIAR, each successive CM was tilted by a vertical half-angle of 0.84 μrad with respect to the previous CM. The beam is launched onto the design curved orbit using the vertical correctors. The curved geometry also results in a finite vertical "design" dispersion of about 1mm in the linac, which must be matched to the incoming beam to prevent beam filamentation.

DISPERSION FREE STEERING

After incorporating the nominal misalignments, one-to-one steering is applied in which the beam is steered, using the vertical corrector magnets, to the center of each BPM. However, this correction scheme is sensitive to BPM-to-quad offsets resulting in dispersive emittance growth.

DFS is one of the steering algorithms which is designed to minimize dispersion and is independent of the BPM-to-quad offsets. For its implementation, the linac is divided into a number of alignment segments with about 40 quads per segment. There is a 50% overlap between segments. BPMs are used to measure two orbits in each segment. The first orbit is measured under nominal conditions while the second orbit is measured by switching off some RF cavities upstream of the segment. The correction is weighted to simultaneously minimize the measured dispersion and the RMS value of the BPM readings. Correction is applied using the corrector magnets.

Figure 1 shows the mean corrected projected emittance growth for 50 random individual machines after incorporating the misalignments given in Table 1 and applying DFS, for both the curved and laser-straight geometry. The same DFS parameters were used in both cases. Figure 1 also shows the corrected emittance dilution distribution for 50 individual machines. It is evident that the emittance growth in a curved linac is very similar to the emittance growth in a straight linac.

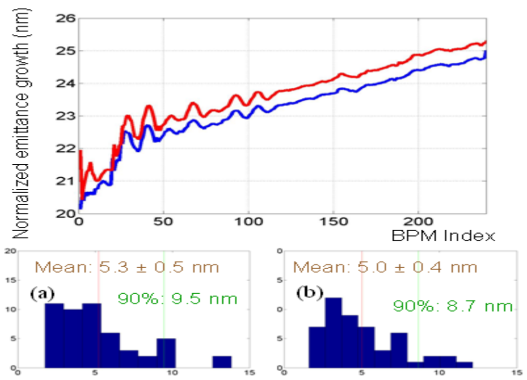

Figure 1: The top plot compares the mean (of 50 random machines) corrected emittance growth for a curved ILC linac (red) and a laser-straight linac (blue) after DFS. The bottom plots show the corrected emittance growth for 50 individual linacs with (a) a curved geometry and (b) a laser-straight geometry.

The sensitivity of the emittance dilution for DFS is investigated for conditions different from the nominal one. Keeping all other misalignments at their nominal values, a given misalignment value is varied and its effect on the emittance dilution of a curved ILC linac is studied. Figure 2 shows that DFS is most sensitive to variations of BPM resolution, cavity pitch, CM offset and quad roll. DFS is found to be almost independent of variations in BPM offset, quad offset, cavity offset, and CM pitch.

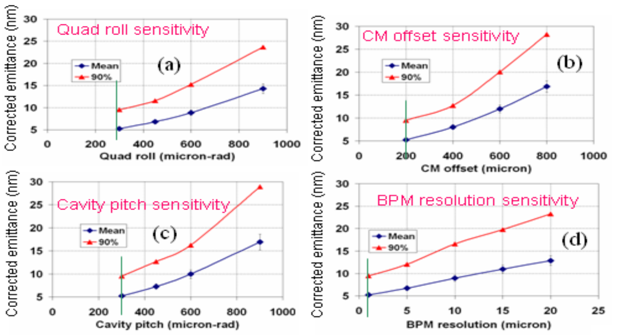

Figure 2: Mean and 90% corrected emittance growth in the ILC curved linac after DFS for different sets of misalignments.

It is observed that the DFS is less sensitive to variations of incoming beam jitter as compared to quad vibration jitter. The effect of a random failed BPM and corrector on the DFS algorithm is also studied. It was found that if we can locate the failed BPM and corrector and exclude it from DFS then the emittance growth in the main linac is similar to that in a linac without a corrector failure.

EMITTANCE BUMPS

Because of the limitations of static tuning techniques, a residual emittance growth takes place in the main linac due to both dispersive and wakefield effects. Although the wakefield effects are in general smaller than the dispersion effects in the main linac of the ILC machine, but, after incorporating various tuning options the residual effects may become comparable. Thus, two different global bumps, dispersion bumps and wakefield bumps, are considered for the present study.

For the dispersion bumps, a closed bump was generated by energizing a pair of correctors 180^0 apart, with appropriate energy scaling for the change in beam energy between the two correctors. In this configuration, dispersive emittance growth continues after the bump. A wire scanner to measure the beam size was placed very close to the end of the main linac, at a D quad and at an F quad 90^0 away. The scan range was set by the bump value needed to double the extracted emittance, given an otherwise perfect linac. For the present case, perfect wire scanner resolution was considered. The bump value was optimized by measuring the beam size at the wire scanners and finding a minimum by fitting the square of the beam size with a parabola. For the wakefield bumps, the methodology is quite similar to dispersion bumps. In this case, the idea is to generate a wakefield dominated effect and globally correct it by measuring the beam size near the end of the linac. We used the same wire scanners and respective locations that were used for the dispersion bumps optimization process. The wakefield bump was generated by placing three correctors 180^0 apart such that the generated dispersion is cancelled after the bumps, and only the wakefield induced emittance growth continues.

Figure 3(a) shows the mean emittance growth in the main linac for 30 independent machines, where one dispersion bump is implemented after incorporating DFS. It is clear that even a single dispersion bump placed near the entrance of the linac helps to significantly reduce the emittance growth when implemented after DFS. Figure 3(b) shows the emittance growth for 30 individual machines. Again, it is observed that a single dispersion bump helps in limiting the emittance growth for all the seeds.

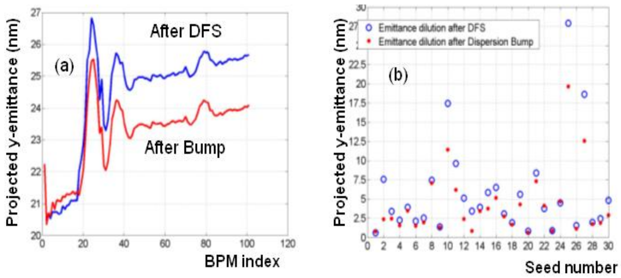

Figure 3: (a) Average projected emittance growth in a nominally misaligned linac for 30 seeds after dispersion free steering, and then implementing a dispersion bump near the entrance of the linac. (b) Results for the individual machines.

It is found that two dispersion bumps are beneficial, but at the same time their respective locations in the linac are also crucial to optimize. Wakefield bumps are also found to be useful in limiting the emittance growth after DFS, indicating the presence of residual wakefield based emittance growth in the linac after static tuning. Figure 4 shows the mean emittance growth in the main linac for 30 independent machines, combining one dispersion and one wakefield bump in the main linac.

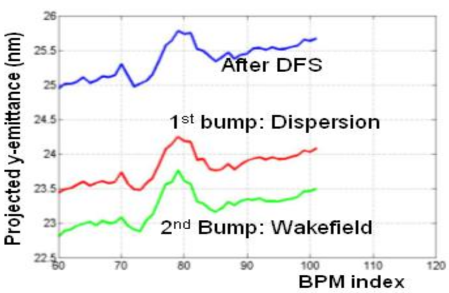

Figure 4: Average projected emittance growth in a nominally misaligned linac for 30 seeds after DFS, and then implementing one dispersion bump at corrector no.3, and one wakefield bump at corrector no. 39.

ADAPTIVE ALIGNMENT

The ground motion in MatLIAR is modeled with a 2-dimensional power spectrum [6], and it includes diffusive ground motion which follows the 'ATL' relation and isotropic plane wave motion. In order to consider different ground motion at various sites, four ground motion models are available in MatLIAR. For the purpose of present studies we considered 50 FODO cells (almost half of the ILC design).

The effectiveness of the adaptive alignment (AA) algorithm as a tuning option is studied. We observe that the adaptive alignment procedure decreases quad offset, smoothes out the beam thrusts, and decreases the emittance growth significantly. However, it is to be noted that the adaptive alignment procedure is sensitive to the BPM centre position w.r.t. the quad centre, and also to the BPM resolution. The effect of BPM resolution can be partially taken care of by optimizing the convergence factor ('gain') and the number of iterations.

A ground motion (GM) model 'C' (relatively noisier model) is chosen and its effect on the main linac is studied. It is found that in the absence of any dynamic tuning, the GM can severely increase the emittance, and hence decrease the luminosity at the interaction point in a few hours.

Figures 5(a) and 5(b) show the normalized emittance plots in the main linac, where nominal values of the static misalignments are chosen for the various elements, and then the linac is statically tuned using DFS. The ground motion of model 'C' is then applied for one hour, and the linac is dynamically tuned using the AA technique. It is found that the AA algorithm can be used effectively to stabilize the emittance growth in the main linac.

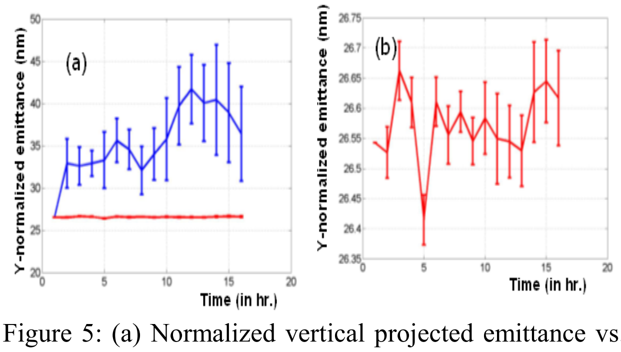

Figure 5: (a) Normalized vertical projected emittance vs. time in a dispersion-free steered linac. AA is implemented after every one hour of GM of model 'C'. (b) A blown-up portion of the plot after AA (100 iterations, gain=0.3).

It is seen that as the BPM resolution increases, the adaptive alignment tends to be less effective for the given convergence factor of 0.3. However, this can be partially taken care of by properly optimizing the convergence factor and the number of AA iterations. As an alternative, an effective BPM resolution can be reduced by summing over a few bunches instead of using a single bunch. It is found that if no alignment is performed then the GM can significantly degrade the performance of the machine in 10 hours.

The Adaptive Alignment algorithm was also studied for the entire ML lattice (114 FODO cells) and a much longer time scale of ~30 days for different GM models. The results are shown in Figure 6. The number of GM seeds used for averaging was limited (from 8 to 10). It shows that AA is still working to effectively keep emittance under control.

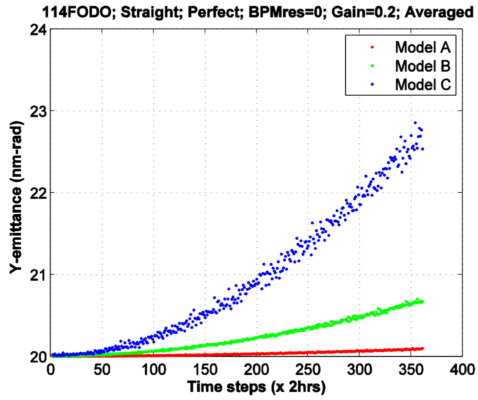

Figure 6: Vertical emittance growth for GM models A, B and C. Convergence = 0.2; 100 AA iterations.

COUPLER RF KICK AND WAKEFIELD

In Lucretia there is an element, TCAV, which works almost exactly like an RF accelerator cavity, except that voltage is applied in transverse plane to deflect the beam. It has been shown elsewhere [7] that RF kick can be implemented by an application of complex voltage instead of applying only real voltage. We have thus implemented RF Kick using same TCAV element, but now with an application of complex voltage.. To include the effect of both upstream couplers & downstream couplers in single TCAV, a net complex voltage is fed to TCAV.

Simulations using Lucretia code were performed in order to estimate the emittance dilution caused by coupler RF kicks. Emittance is calculated for various cases in main linac. Real kick doesn't depend on longitudinal position of the particle within bunch and hence corresponding kick remains same for the whole bunch. This emittace dilution can be corrected using one-to-one (1:1) correction mechanism. In contrast Imaginary kick depends on the longitudinal position of particle within bunch so it will vary according to the position of particle within bunch and corresponding emittance dilution can not be compensated using one to one correction. In Figure 7 both real and imaginary parts of the voltages are applied to TCAV & effect is also studied after 1:1 correction. These results are consistent with analytical calculations.

SUMMARY

The beneficial effects of implementing emittance bumps after dispersion free steering for the proposed ILC machine is described. Because of the presence of residual emittance growth from dispersion and wakefield related emittance growth after static tuning, these global bumps are found to be very important to further limit the emittance growth.

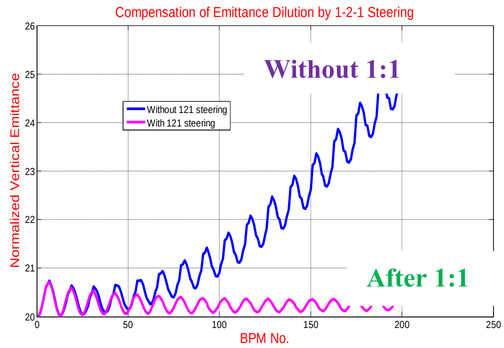

Figure 7: Emittance behaviour of the beam in Main Linac when both real & imaginary part of kick voltage (**V: -7.3+ i 11.1**) is applied to TCAV.

To the first approximation, transverse kick neither depends on transverse coordinates of incident particle nor on the transverse coordinate of witness particle, so for fixed longitudinal charge distribution along bunch, transverse wake profile versus 's' is fixed, where 's' is position of particle within the bunch.

We have investigated the effect of the GM on the emittance dilution performance of the main linac on a time scale of ~ month. It is found that in the absence of any dynamic steering GM can severely limit the emittance dilution performance. It is also observed that an AA algorithm can be helpful as a dynamic tuning technique to stabilise the emittance performance in a perfect or DFS linac. We have also implemented couplers' effects, both RF kicks and wake-fields, in beam dynamics program, Lucretia. It is found that 1:1 correction mechanism can be used to limit emittance growth for RF kicks induced by real component of applied voltage. We have also implemented coupler wake field, and checked its corresponding effect on beam trajectory.

REFERENCES

[1] T. Raubenheimer and P. Tenenbaum, LCC-0129, LCC Tech. Notes, 2003
[2] A. Alexandrov, V. Balakin, A. Lunin, Proc. of the LINAC'96 Conf., p.255, Geneva (1996).
[3]http://www.linearcollider.org/wiki/doku.php?id=bcd:bcd_home
[4]http://www.slac.stanford.edu/accel/nlc/local/AccelPhysics/codes/liar/web/liar.htm
[5] P. Tenenbaum, PAC'05, Knoxville, 2005, p. 4197.
[6] P. Tenenbaum, L. Hendrickson, A. Seryi, G. Stupakov, Proc. of the EPAC'02 Conf., p.518, Paris (2002).
[7] N.Solyak et al, "RF Kick in the ILC Acceleration Structure", MOPP042 (EPAC 08).